J Mater Sci: Mater Med (2007) 18:661–668
DOI 10.1007/s10856-007-2317-1

Mechanical properties and apatite forming ability of TiO_2 nanoparticles/high density polyethylene composite: Effect of filler content

Masami Hashimoto · Hiroaki Takadama · Mineo Mizuno · Tadashi Kokubo

Received: 23 December 2004 / Accepted: 21 October 2005

Abstract Composite materials consisting of TiO_2 nanoparticles and high-density polyethylene (HDPE), designated hereafter as TiO_2/HDPE, were prepared by a kneading and forming process. The effect of TiO_2 content on the mechanical properties and apatite forming ability of these materials was studied. Increased TiO_2 content resulted in an increase in bending strength, yield strength, Young's modulus and compressive strength (bending strength = 68 MPa, yield strength = 54 MPa, Young's modulus = 7 GPa, and compressive strength = 82 MPa) at 50 vol% TiO_2. The composite with 50 vol% TiO_2 shows a similar strength and Young's modulus to human cortical bone. The TiO_2/HDPE composites with different TiO_2 contents were soaked at 36.5 °C for up to 14 days in a simulated body fluid (SBF) whose ion concentrations were nearly equal to those of human blood plasma. The apatite forming ability, which is indicative of bioactivity, increased with TiO_2 content. Little apatite formation was observed for the TiO_2/HDPE composite with 20 vol% content. However, in the case of 40 vol% TiO_2 content and higher, the apatite layers were formed on the surface of the composites within 7 days. The most potent TiO_2 content for a bone-repairing material was 50 vol%, judging from the mechanical and biological results. This kind of bioactive material with similar mechanical properties to human cortical bone is expected to be useful as a load bearing bone substitute in areas such as the vertebra and cranium.

M. Hashimoto · H. Takadama (✉) · M. Mizuno
Japan Fine Ceramics Center, 2-4-1 Mutsuno, Atsuta-ku, Nagoya 456-8587, Japan
e-mail: masami@jfcc.or.jp

T. Kokubo
Research Institute for Science and Technology, Chubu University, 1200 Matsumoto-cho, Kasugai 487-8501, Japan

Introduction

It has been reported that some ceramics, such as Na_2O-CaO-SiO_2-P_2O_5 glasses [1], sintered hydroxyapatite [2], and glass-ceramics containing crystalline apatite and wollastonite (A–W) [3], can bond to living bone. These ceramics are already clinically used as important bone-repairing materials. Recently, it was also reported that even metals such as titanium and its alloys can bond to living bone when they have been previously subjected to alkali and heat treatment [4] or alkali, water and heat treatment [5]. However, they have much higher elastic moduli than does natural bone. This is a critical problem, since a high elastic modulus of the materials may induce bone resorption because of their stress shielding. On the other hand, polymeric materials generally possess low elastic moduli, but none bond to living bone except for Polyactive™, which is biodegradable [6]. Therefore, new types of materials having a high bioactivity as well as mechanical strengths analogous to those of the natural bone must still be developed for load-bearing bone substitutes.

A composite (HAPEX™) of hydroxyapatite particles with high-density polyethylene (HDPE) was developed in the early 1980s as a bone substitute with analogous mechanical properties to those of the bone [7]. It is already clinically used for artificial incus bones. Some of the mechanical properties of HAPEX™, such as the tensile strength, have already been found to be desirable for its use in the body [8–10]. However, the fracture toughness and elastic modulus of HAPEX™ are lower than those of living bone. Additionally, glass – ceramic A-W-reinforced HDPE was developed in 1998 [11, 12]. The bioactivity of this composite is higher than that of HAPEX™, but its mechanical strengths are lower than that of HAPEX™.

On the other hand, hydroxyapatite-reinforced poly–(L-lactide) (PLLA) [13] has an initial bending strength of

280 MPa, which exceeds the bending strength of the human cortical bone (50 to 150 MPa), and an elastic modulus of 12 GPa, which is in the range of the elastic modulus of the human cortical bone (7 to 30 GPa) [14]. These mechanical properties of this composite, however, decrease to 200 MPa after 25 weeks in the phosphate-buffered saline because of the biodegradability of PLLA. Therefore, this composite is not useful as a load-bearing bone substitute but only for fracture-fixation devices such as pins or screws. Therefore, in order to develop a bone-repairing material with bone-like mechanical properties, it is necessary to incorporate a bioactive ceramic particulate with a high mechanical strength and elastic modulus into a nondegradable ductile matrix.

Kokubo et al. reported that titania gels with an amorphous structure did not induce apatite formation on their surfaces in a simulated body fluid (SBF), which was prepared to have an ion concentration nearly equal to that of human blood plasma (Na^+ 142.0, K^+ 5.0, Ca^{2+} 2.5, Mg^{2+} 1.5, Cl^- 147.8, HCO_3^- 4.2, HPO_4^{2-} 1.0, and SO_4^{2-} 0.5mM) [15], whereas the gels with an anatase or rutile structure induced apatite formation on their surfaces [16–18]. The deposition of apatite was more pronounced on the anatase gels than on the rutile gels. Therefore, a titania with a specific crystal structure, such as anatase, is effective in inducing apatite nucleation in a body environment.

Fillers have an important role in modifying the properties of various polymers. In polymeric materials, inorganic particles are used as fillers to improve their strength, toughness and wear properties [19]. The effect of fillers on the properties of the composites depends on their concentration and particle size and shape, as well as their interaction with the matrix. As yet, there has been no study regarding the effect of TiO_2 on the mechanical strengths of HDPE. TiO_2 has high mechanical strengths. For example, the elastic modulus of TiO_2 (300–320 GPa) is much higher than that of hydroxyapatite (86–110 GPa) [14]. So incorporating TiO_2 particles into the polymer matrix is considered to be effective to enhance the mechanical properties of the polymer matrix.

In this study, the effects of TiO_2 content on the bending, yield strengths, Young's modulus, the strain to failure, and compressive strength of TiO_2/HDPE composite were investigated. In addition, the apatite forming ability of TiO_2/HDPE composite in SBF was studied.

Materials and methods

Materials

Solvents and reagents, all of special reagent grade, were used without further purification. An anatase-type TiO_2 nanopowder was manufactured by Ishihara Sangyo Kaisha, Ltd., Mie, Japan. The phase of the TiO_2 powders was analyzed by powder X-ray diffraction. The TiO_2 particles were analyzed in terms of size using a laser scattering particle size distribution analyzer (MasterSizer 2000, MALVERN Co., Japan) and a BET–specific surface area analyzer (NOVA-2000, Yuasaionics Co., Japan). The surface chemical composition of the outermost layer of the as-received TiO_2 was analyzed by an X-ray photoelectron spectrometer (XPS) with an ESCA LAB MKII Model (VG Scientific, East Grin stead, England). An MgKα X-ray was used as the source. The photoelectron take–off angle was set at 30°. The measured binding energy was corrected by referring to that of the C1s as 285.0 eV. The zeta potential of the surface of the as-received TiO_2 was measured by laser electrophoresis with a Penmkem 501 Model in 0.01 mol/l phosphate buffer saline of pH 7.2 at 20 °C.

HDPE (Japan Polyolefins Co., Ltd., Tokyo, Japan) had the following number-average molecular weight: Mn, weight-average molecular weight in 1.2×10^4; Mw in 7.67×10^4 and z-average molecular weight; Mz in 47.6×10^4, Mw/Mn in 6.35 and Mz/Mw in 6.20. The melt flowing rate (MFR) of this polyethylene is 8.

Preparation of TiO_2/HDPE composites

The manufacturing process of the TiO_2/HDPE involved kneading and compression moulding. The filler content was set at 20, 40, 45, 50, 52, 52.5 and 55.6 vol%. These composites were denoted as TiO_2/HDPE −20, 40, 45, 50, 52, 52.5 and 55.6, respectively. HDPE was dried at 80 °C for 8 h and then kneaded at 210 °C in a batch kneader PBV 0.3 (Irie Seisaku-sho, Ltd., Tokyo, Japan). TiO_2 particles were added slowly into the melted HDPE with kneading at 210 °C in air. After adding TiO_2, the TiO_2/HDPE compound was kneaded with a 25 rpm rotation speed for 30 min.

The obtained compounds were molded at 230 °C for 1 h and then hot-pressed in air under a pressure of 2.5 MPa.

Characterization of TiO_2/HDPE composites

Mechanical test

Three-point bend testing of TiO_2/HDPE composites was performed using ten samples of each type of composite. The specimens were cut to the desired shape and then polished, using 400 grit silicon carbide paper, to a size of 40 mm × 10 mm × 4 mm. A testing machine, Model 5582 (Instron Co. Ltd., L. A., USA), was used to apply a load over a 30 mm span. Measurements were performed with a cross–head speed of 1.0 mm/min at room temperature according to JIS K 7171. The fracture surfaces were examined using a field emission scanning electron microscope (FE-SEM)

with a JSM-633OF Model (JEOL DATUM Co. Ltd., Nagoya, Japan) after coating with a thin layer of Au.

The values for bending strength, Young's modulus, yield strength and strain to failure were calculated according to the following equations: [12, 20]

$$\text{Bending strength } \sigma = 3pL/2bd^2 \quad (1)$$

$$\text{Young's modulus E } = \sigma/(6d\delta/L^2) \quad (2)$$

$$\text{Yield strength } \sigma_f = (3p_fL/2bd^2)((n+2)/3) \quad (3)$$

$$\text{Strain to failure } \varepsilon = (6d\delta/L^2)((2n+1)/n)(1/3), \quad (4)$$

where p is the load at elastic limit (N), p_f is the load at fracture (N), L is the sample length (mm), δ is the displacement of the cross head (mm), b is the sample width (mm), d is the sample height (mm) and n is a strain-hardening exponent ($0 < n < 1$).

For compressive mechanical analysis, specimens of the dimensions 10 mm × 10 mm × 4 mm were cut from the hot-pressed composite plates. They were subsequently polished using 400 grit silicon carbide papers to remove defects from the specimen surfaces. The strength measurement was carried out at a cross–head speed of 1.0 mm/min according to JIS K 7181. The tests were carried out at room temperature in air.

The compressive strength was calculated from

$$\text{Compressive strength, } \sigma_f = F/A, \quad (5)$$

where F is fracture load (N) and A is the initial cross sectional area (mm^2).

Density

The densities of the TiO_2/HDPE composites were measured by the Archimedes method using a pycnometer and a glass bottle of known volume with a capillary tube at the top as a container. The liquid medium for all materials was distilled water.

Bioactivity test

The bioactivity of the TiO_2/HDPE composites was evaluated by examining apatite formation on their surfaces in the simulated body fluid (SBF). It has been revealed that materials that form a bone-like apatite on their surfaces in SBF form the apatite even in a living body and bond to living bone through the apatite layer [21]. The bioactivity of the composite was compared with that of TiO_2 particles or pure HDPE. The TiO_2 particles were embedded on the tape stuck to a glass slide 10 mm × 10 mm × 2 mm in size. For both HDPE and TiO_2/HDPE composites, specimens of 10 mm × 10 mm × 4 mm in size were cut, polished with a 400 grit silicon carbide paper for 5 min, washed with distilled water and dried at room temperature. SBF with ion concentrations nearly equal to those of human blood plasma was prepared by dissolving the reagents NaCl, $NaHCO_3$, KCl, $K_2HPO_4{\cdot}3H_2O$, $MgCl_2{\cdot}6H_2O$, $CaCl_2$ and Na_2SO_4 (Nacalai tesque, Inc. Kyoto, Japan) in distilled water and buffered at pH7.4 and 36.5 °C with $(CH_2OH)_3CNH_2$ and 1M HCl (Nacalai tesque, Inc. Kyoto, Japan). The specimens were soaked in 30 ml of SBF at 36.5 °C. After various time periods, the specimens were removed from the fluid, washed moderately with ion-exchanged distilled water, and dried at room temperature for 1 day. Their surfaces were analyzed by thin-film X-ray diffraction (TF-XRD) with RINT Model 2000 (Rigaku Denki Co. Ltd., Tokyo, Japan). The morphology of the surface layer of the composites was observed by FE-SEM after coating them with a thin Au film.

Results

Characterization of TiO_2

The as-received TiO_2 particles were confirmed to be essentially of the anatase phase by powder X-ray diffraction analysis. They had a broad particle size distribution, with a median particle size of 535 nm. The BET surface area of the as-received TiO_2 was approximately 8.56 m^2g^{-1}. Figure 1 shows a TEM photograph of the as-received TiO_2. TiO_2 particles possessed a round shape and smooth surface. Figure 2 shows O(1s) spectra of the as–received TiO_2. Both TiO_2 and Ti-OH peaks were detected. This result indicates that the as-received TiO_2 already has Ti-OH groups, which is essential for apatite nucleation. The zeta potential of the surface of the as-received TiO_2 was found to be highly negative (−22.5 mV).

Fracture surface of composites

Figure 3 shows FE-SEM images of the fracture surfaces of TiO_2/HDPE composites with different TiO_2 contents after the bending test. As the FE-SEM image in Fig. 3a shows, at 20 vol% filler content there was a large degree of polymer deformation; this was indicated by the presence of elongated strands of polyethylene. However, with greater than 40 vol% of TiO_2 (Figs. 3b,c and d), there was a small degree of polymer deformation. Along with the formation of polymer fibrils, the particles of TiO_2 were still clearly seen within the polyethylene matrix. It was easy to detect the TiO_2 agglomerates in the TiO_2/HDPE-52 (Fig. 3c) and TiO_2/HDPE-56 (Fig. 3d).

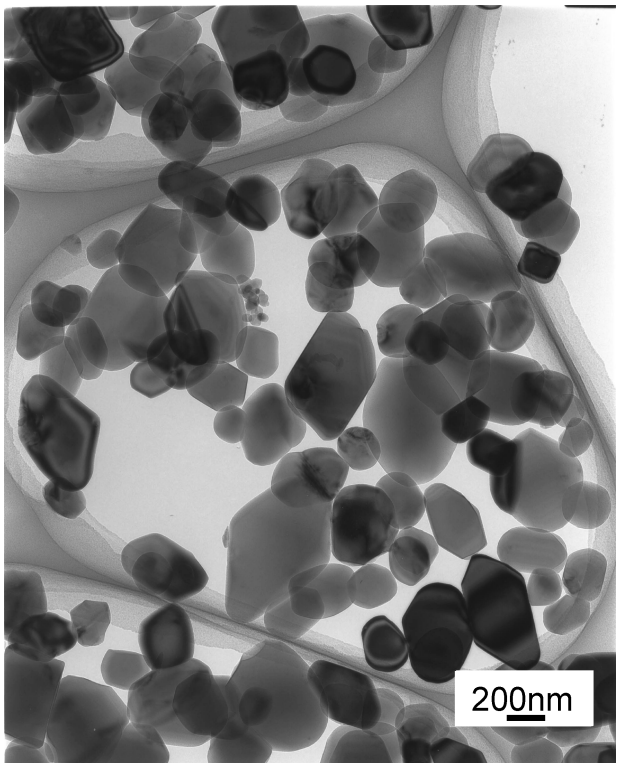

Fig. 1 Transmission electron micrograph of the as-received TiO_2 particles

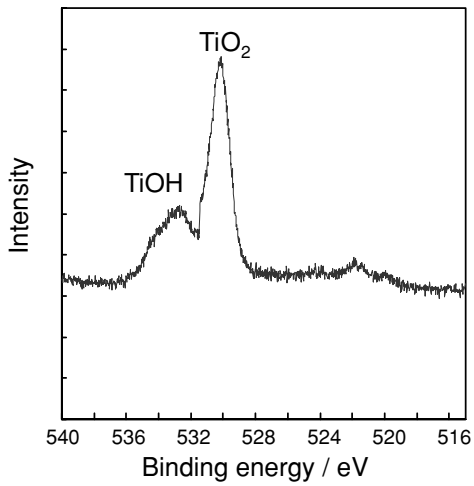

Fig. 2 O(1s) peak in the XPS spectrum of as-received TiO_2

Mechanical properties of composites

The values for bending strength, yield strength, Young's modulus, fracture strain and compressive strength of the TiO_2/HDPE composites and HDPE are shown in Table 1. The bending strength, yield strength and Young's modulus increased with increasing TiO_2 content up to 50 vol% and decreased with increasing content above 52 vol%. The yield strength and Young's modulus were, respectively, 28 MPa and 1.4 GPa for HDPE, 49 MPa and 7.6 GPa for TiO_2/HDPE-40, 54 MPa and 7.1GPa for TiO_2/HDPE-50, and 29 MPa and 6.8 GPa for TiO_2/HDPE-55.6. The strain to failure decreased as the TiO_2 content increased up to 40 vol%. However, the values obtained for the strain to failure increased for the composites with a TiO_2 content higher than 45 vol%.

The increase in the TiO_2 volume fraction resulted in an increase in compressive strength. The following compressive strengths were obtained: 22 MPa for HDPE, 61 MPa for TiO_2/HDPE-40, 75 MPa for TiO_2/HDPE-50, and 87 MPa for TiO_2/HDPE-55.6.

The representative load-displacement curves of three-point bend testing were demonstrated for TiO_2/HDPE composites in Fig. 4. Figure 4 shows that HDPE did not fracture within the limits of the three-point bending apparatus. This behavior resulted in mechanical properties, in that they had a low bending strength, yield strength and Young's modulus, and a large strain to failure. For TiO_2/HDPE-20 and TiO_2/HDPE-40, this ductile behavior was no longer a dominant feature. As the TiO_2 content increased from 40 vol%, the fracture strain also increased.

Density of composites

Figure 5 shows the densities of TiO_2/HDPE composites. Compared to the theoretical density, which was calculated by the rule of mixture, the density of TiO_2/HDPE composites with a low TiO_2 content (20 vol%) almost matched the theoretical value. However, as the amount of TiO_2 was increased up to 55.6 vol%, the discrepancy between the measured and theoretical densities increased.

Bioactivity of composites

Figure 6 shows TF-XRD patterns of TiO_2 particle (a) and HDPE (b) which were soaked in SBF for 3 and 14 days, respectively. Apatite was able to form on the TiO_2 particles after 3 days of soaking; however, it was not formed on the HDPE even after 14 days of soaking in SBF.

Figure 7 shows TF-XRD patterns of TiO_2/HDPE composites that were soaked in SBF for 14 days. Apatite peaks were detected on all of the TiO_2/HDPE composites except for those with 0 and 20 vol% of TiO_2. This result indicates that the apatite forms on TiO_2/HDPE composites with a TiO_2content greater than 40 vol% in SBF and that apatite-forming ability increases with increasing TiO_2 content. Figure 8 shows TF-XRD patterns of a TiO_2/HDPE composite with 50 vol% of TiO_2 that was soaked in SBF for various periods up to 14 days. Small apatite peaks were detected at 7 days of soaking. With 14 days of soaking, these apatite peaks increased. This result indicates that the apatite formed on a TiO_2/HDPE composite with 50 vol% of TiO_2 increased with increasing soaking time.

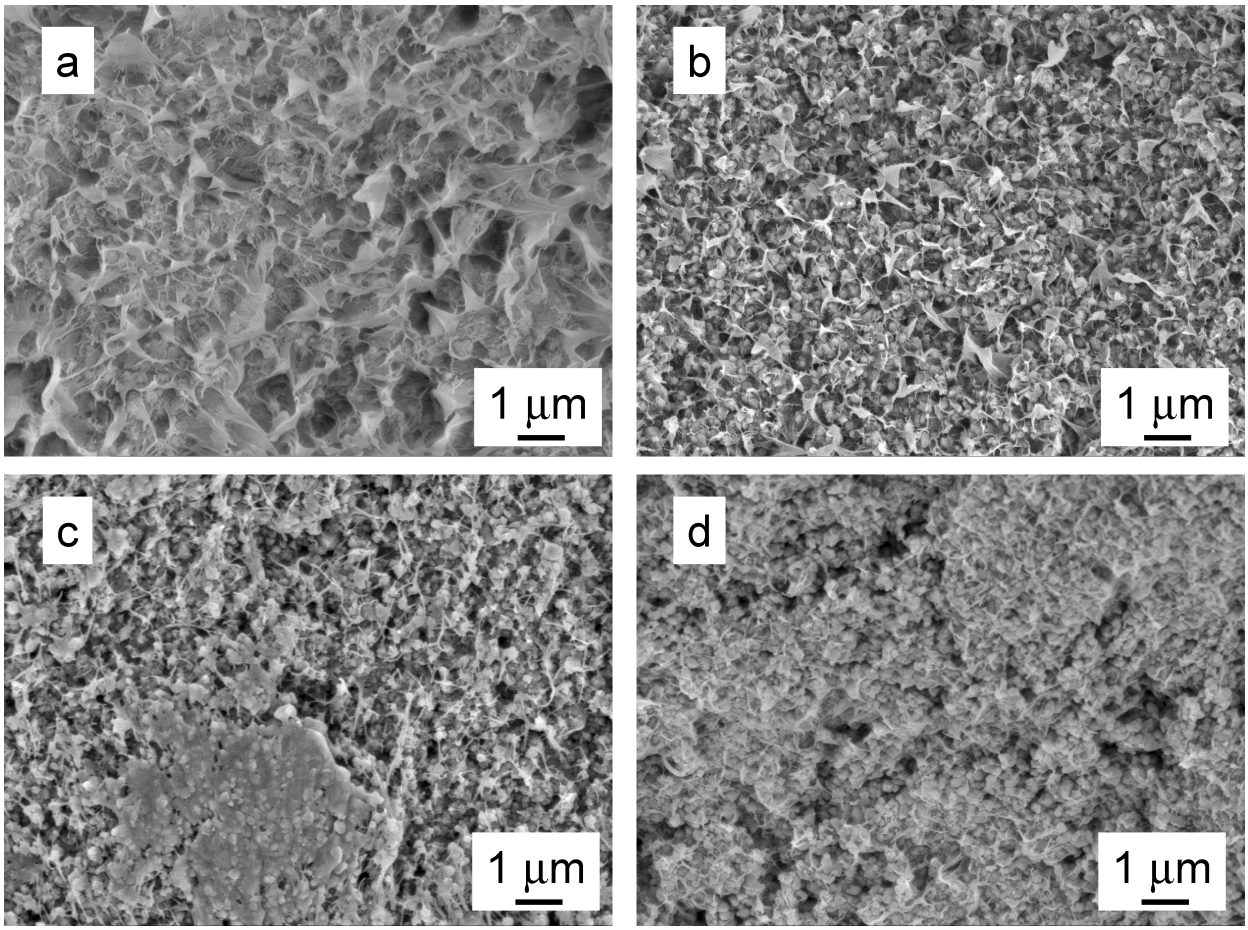

Fig. 3 Scanning electron micrographs of fracture surfaces of TiO_2/HDPE composites −20 (a), 40 (b), 52 (c) and 55.6 vol% (d)

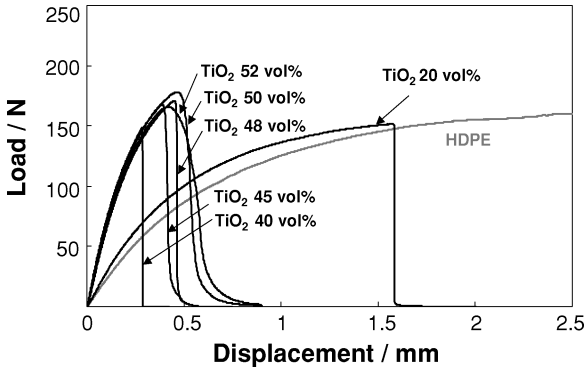

Fig. 4 Load-displacement curves for TiO_2/HDPE composites

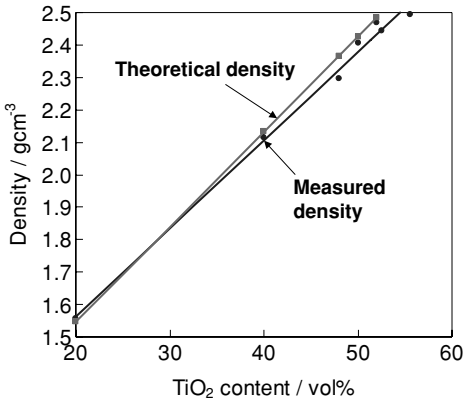

Fig. 5 Density of TiO_2/HDPE composites as a function of the TiO_2 content

Figure 9 shows FE-SEM photographs of the TiO_2/HDPE composite with 50 vol% of TiO_2 that was soaked in SBF at 36.5 °C for various periods shorter than 14 days. No crystals were formed on the TiO_2/HDPE (Fig. 9b) surfaces after soaking in SBF for 5 days. The TiO_2/HDPE surface was covered with hemispherical particles around several micrometers in diameter after 7 days of soaking in SBF (Fig. 9c), and the number and size of the apatite nuclei increased with increasing soaking time (Fig. 9d). The morphology of the apatite on the TiO_2/HDPE composite was polycrystalline fine particles.

Discussion

The results shown here demonstrate that only the 20 vol% TiO_2 incorporation into the HDPE matrix was effective in enhancing the mechanical strengths of the HDPE. The reason for this effect is that the high mechanical strength of TiO_2 (Young's modulus 300–320 GPa) and its smaller particle size allow for a greater surface area to be available

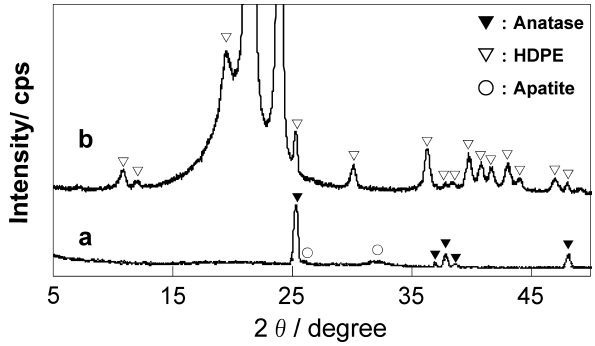

Fig. 6 TF-XRD patterns of the surfaces of TiO_2 particles (a) and HDPE (b) soaked in SBF at 36.5 °C for 3 and 14 days, respectively

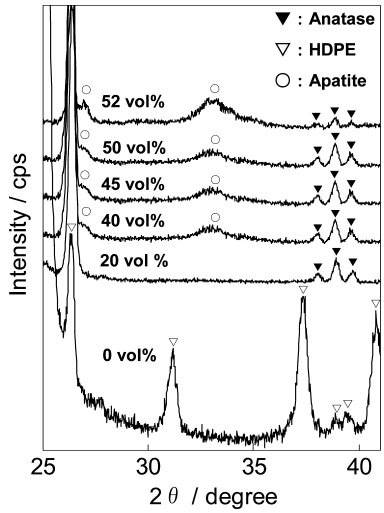

Fig. 7 TF-XRD patterns of the surfaces of TiO_2/HDPE –x composites soaked in SBF at 36.5 °C for 14 days (X = 0, 20, 40, 45, 50, 52 vol%)

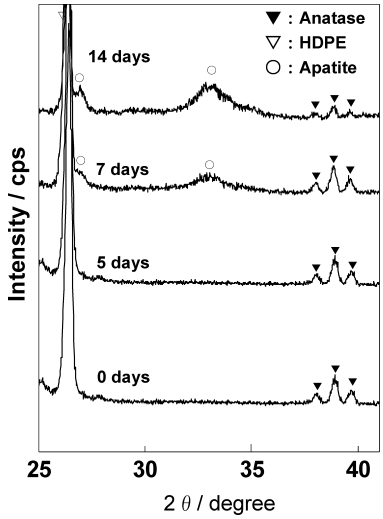

Fig. 8 TF-XRD patterns of the surfaces of TiO_2/HDPE-50 soaked in SBF at 36.5 °C for various periods

for polymer/filler interaction and adhesion. The bending strength, yield strength and Young's modulus increased with increasing filler content, but they decreased when the filler content was greater than 52 vol%. Achieving a homogeneous dispersion of nanoparticles in a polymeric matrix is very difficult due to the strong tendency of nanoparticles to agglomerate [22]. Consequently, nanoparticle–filled polymers are liable to form a number of loosened clusters of particles. Figures 3c and d show TiO_2 aggregate in the HDPE matrix. These agglomerated for the composites with a TiO_2 content greater than 52 vol% and decreased the bending strength, yield strength and Young's modulus.

TiO_2/HDPE-20 and −40 also exhibited a much smaller plastic region after yielding, indicating that the interfacial bond between TiO_2 and HDPE was weak. As mentioned previously, TiO_2 nanoparticles (Fig. 1) had loosened clusters created by the aggregation of smaller TiO_2 particles this is shown in Figs. 3c and d. This structure caused a higher strain to failure due to an increase in crack deflection with increasing particle size of the composite with larger than 40 vol% TiO_2. For TiO_2/HDPE composites, no residual polyethylene was found on the TiO_2 particle surfaces, indicating that no chemical bond existed between the matrix and filler (Fig. 3). Therefore, the voids form at the particle matrix interface, first in the direction of the applied stress (Fig. 5). This void then grows and merges as shear stresses deform the rest of the matrix, leading to the eventual failure of the composites. This result is consistent with the model proposed by Juhasz et al. for an apatite-wollastonite reinforced HDPE composite with no interfacial bonding [12].

Bonfield et al. developed hydroxyapatite-reinforced HDPE composite (HAPEX^{TM}) as an analogue material for bone replacement [7–10].The closer Young's modulus matching of the material to bone is an important factor in solving the problem of bone resorption. The fracture toughness and Young's modulus of HAPEX^{TM} have a lower value than those of the human cortical bone.

The yield strength (50 MPa) and Young's modulus (7 GPa) for TiO_2/HDPE-40 were much larger than those for the HAPEX^{TM} with 40 vol % of hydroxyapatite (28 MPa and 4.1 GPa, respectively). It has been generally observed that the addition of ceramic filler can substantially improve the mechanical strengths of the polyethylene. The mechanism of the reinforcing action is as follows. Inorganic fillers are actually bonded to the macromolecular chains and thereby immobilize the polymer chains. The degree of adhesion between the polymer matrix and fillers, the surface area of the filler, and the packing characteristics of the filler particles are important factors that determine the mechanical properties of the composites [23–25]. Comparing TiO_2 with hydroxyapatite as a ceramic filler, the surface area (8.56 m^2g^{-1}) and average particle size (535 nm) of TiO_2 were much larger and lower than those of hydroxyapatite [7] (7.61 m^2g^{-1} and 7.3 μm, respectively). TiO_2(40 vol%) homogeneously dispersed in the HDPE matrix via the kneading and compacting of TiO_2

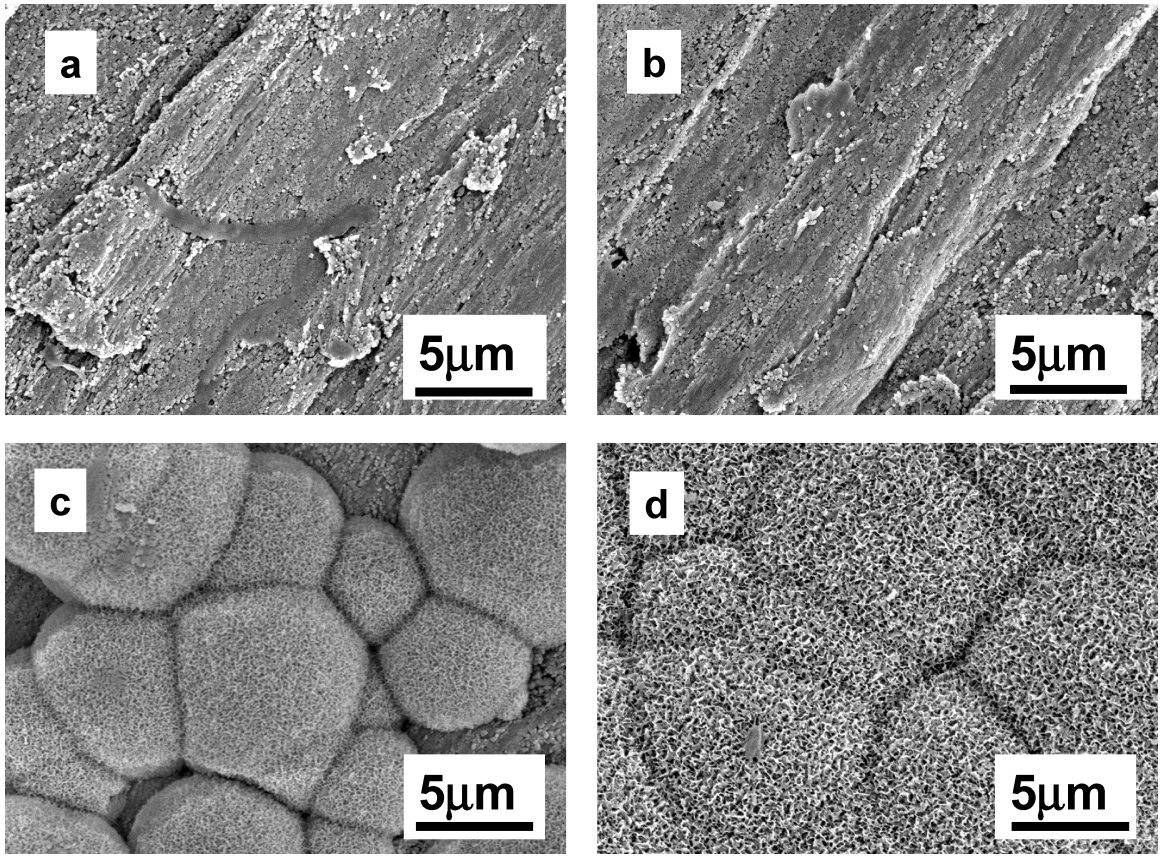

Fig. 9 Scanning electron micrographs of the surfaces of the TiO_2/HDPE-50 composite soaked in SBF at 36.5 °C for various periods: 0 days (a), 5 days (b), 7 days (c) and 14 days (d)

nanoparticles and HDPE (Fig. 3b). Many kinds of polyethylene exist, including ultrahigh molecular weight polyethylene (UHMWPE), HDPE and low density polyethylene (LDPE). Our previous study indicated that the degree of TiO_2 nanoparticle dispersion in the various polyethylene matrixes varied [26–28]. Therefore, the degree of homogeneous dispersion decreased in the order: HDPE (MFR8) > HDPE (MFR20) $\gg$ HDPE (MFR0.3) $\simeq$ HDPE (MFR40) $\gg$ UHMWPE $\simeq 0$. These results indicate that the HDPE (MFR8) matrixes, in which TiO_2 nanoparticles with a high surface area are homogeneously dispersed have high mechanical properties, and that those with micrometer–sized hydroxyapatite particles eventually have low ones.

Biomineralization processes such as apatite formation are complex and involve the controlled nucleation and growth of apatite from aqueous solutions. Organisms create the proper organic matrix as a host for nucleation and growth, for control of solution concentrations, and for the supersaturation of precipitating phases. Most of the macromolecules known to promote surface nucleation contain functional groups that are negatively charged at pH's where the crystallization occurs [29].

In general, the crystallization of many sparingly soluble salts involves the formation of metastable precursor phases. In the case of calcium phosphate, various metastable phases have been identified. It is believed that the initial formation of an amorphous calcium phosphate may be followed by its transformation to hydroxyapatite. A recent X-ray diffraction crystallographic study by Kokubo showed that the anatase gel induces apatite formation the most effectively, followed by the rutile gel; the amorphous gel, however, forms no apatite [18]. The Ti-OH groups on the anatase gel combine with Ca^{2+} ions in the SBF to form amorphous calcium titanate. This calcium titanate later combines with phosphate ions in the SBF to form amorphous calcium phosphate with a low Ca/P ratio [30, 31]. The calcium phosphate transforms into the apatite, which exhibits a Ca/P ratio of 1.65. This demonstrates that the surface functional groups, which are capable of binding soluble ionic precursors, may become sites for surface nucleation.

The XRD study showed that the apatite formed on all the TiO_2/HDPE composites except for those with 0 and 20 vol % of TiO_2, as exemplified by the composite with 52 vol% of TiO_2 shown in Fig. 7. The induction period of the apatite nucleation was 7 days, as shown in Fig. 8. The as-received TiO_2 has an anatase structure, a Ti-OH group (Fig. 2) and a negative zeta potential (−22.5 mV). Figure 6 shows the apatite formed on the TiO_2 particles after soaking in SBF for as

little as 3 days; however no apatite formed on the polyethylene after soaking in SBF for 14 days. The TiO_2/HDPE surfaces were ground to a 30 μm finish with #400 silicon carbide abrasive paper. This suggests that the HDPE polymer chains were elongated and partially covered the surfaces of the TiO_2 particles. Therefore, the induction period of the apatite formation would be delayed for a longer time than that for TiO_2 particles. To enhance the apatite forming ability of the TiO_2/HDPE composite, it is necessary to remove by surface treatment the polyethylene that covers the TiO_2 particles.

Conclusions

The bending strength, yield strength, Young's modulus and compressive strength increased with increasing TiO_2 content up to 52 vol% (maximum bending strength = 68 MPa, yield strength = 54 MPa, Young's modulus = 7 GPa and compressive strength = 82 MPa). The strain to failure was reduced with increasing TiO_2 up to 40 vol%. However, as the filler content was increased from 45 to 52 vol%, the strain to failure increased due to the larger particle size resulting from the aggregation of TiO_2 nanoparticles. Three–point bending and compressive testing demonstrated that the composites with a filler content between 40 and 50 vol% showed the most suitable mechanical properties for maxillofacial applications. Apatite formed on TiO_2/HDPE that had greater than 40 vol% of TiO_2 after soaking in SBF for 7 days. These results indicate that the TiO_2/HDPE-50 composite is the most promising material in the present study for use as a load–bearing bone substitute.

Acknowledgements This work is in part supported by the National Research & Development Programs for Medical and Welfare apparatus from the New Energy and Industrial Technology Development Organization (NEDO) entrusted to the Japan Fine Ceramics Center.

References

1. L. L. HENCH, R. J. SPLINTER, W. C. ALLEN and T. K. JR. GREENLEE, *J. Biomed. Mater. Res*. **2** (1971) 117.
2. M. JARCHO, J. L. KAY, R. H. GUMAER and H. P. DROBECK, *J. Bioeng*. **1** (1977) 79.
3. T. KOKUBO, M. SHIGEMATSU, Y. NAGASHIMA, M. TASHIRO, T. NAKAMURA, T. YAMAMURO and S. HIGASHI, *Bull. Inst. Chem. Res. Kyoto Univ*. **60** (1982) 260.
4. S. NISHIGUCHI, H. KATO, H. FUJITA, H. M. KIM, F. MIYAJI, T. KOKUBO and T. NAKAMURA, *J. Biomed. Mater. Res*. **48(5)** (1999) 689.
5. S. FUJIBAYASHI, T. NAKAMURA, S. NISHIGUCHI, J. TAMURA, M. UCHIDA, H. M. KIM and T. KOKUBO, *J. Biomed. Mater. Res.* **56(4)** (2001) 562.
6. C. A. VAN BLITTERSWIJK, D. BAKKER, H. LEENDERS, J. BRINK, S. C. HESSELING, Y. P. BORELL, A. M. RADDER, R. J. SAKKERS, M. L. GAILLARD, P. H. HEINZE and G. J. BEUMER, ed. by P. Ducheyne, T. Kokubo and C. A. Van Blitterswijk, (Reed Healthcare Communications, The Netherlands, 1992) p. 13.
7. W. BONFIELD, M. D. GRYNPAS, A. E. TULLY, J. BOWMAN and J. ABRAM, *Biomaterials* **2** (1981) 185.
8. M. WANG, R. JOSEPH and W. BONFIELD, *Biomaterials* **19** (1998) 2357.
9. M. WANG and W. BONFIELD, *Biomaterials* **22** (2001) 1311.
10. M. WANG, *Biomaterials* **24** (2003) 2133.
11. J. A. JUHASZ, S. M. BEST, W. BONFIELD, M. KAWASHITA, N. MIYATA, T. KOKUBO and T. NAKAMURA, *J. Mater. Sci: Mater. In Med*. **14** (2003) 489.
12. J. A. JUHASZ, S. M. BEST, R. BROOKS. M. KAWASHITA, N. MIYATA, T. KOKUBO, T. NAKAMURA and W. BONFIELD, *Biomaterials* **25** (2004) 949.
13. T. FURUKAWA, Y. MATSUSUE, T. YASUNAGA, Y. NAKAGAWA, Y. OKADA, Y. SHIKINAMI, M. OKUNO and T. NAKAMURA, *J. Biomed. Mater. Res*. **50** (2000) 410.
14. L. L. HENCH and J. WILSON, in "An introduction to bioceramics" (World Scientific Publishing Co, London, 1992) p. 12.
15. T. KOKUBO, H. KUSHITANI and S. SAKKA, *J. Biomed. Mater. Res*. **24** (1990) 721.
16. M. UCHIDA, H. M. KIM, T. KOKUBO and T. NAKAMURA, *J. Am. Ceram. Soc*. **84** (2001) 2969.
17. M. WEI, M. UCHIDA, H. M. KIM, T. KOKUBO and T. NAKAMURA, *Biomaterials* **23** (2002) 167.
18. M. UCHIDA, H. M. KIM, T. KOKUBO and T. NAKAMURA, *J. Biomed. Mater. Res*. **64A** (2003) 164.
19. T. P. SELVIN, J. KURUVILLA and T. SABU, *Materials Letters* **58** (2004) 281.
20. N. E. DOWLING, in "Engineering materials for deformation, fracture and fatigue" (Prentice-Hall Inc, Englewood Cliffs, NJ; 1993). p. 570.
21. T. NAKAMURA, M. NEO and T. KOKUBO, in "Mineralization in Natural and Synthetic Biomaterials" ed. by P. Li, P. Calvert, T. Kokubo, R. Levy and C. Sheid (Materials Research Society, Warrendale, PA, 2000) p.15.
22. M. Z. RONG, M. Q. ZHANG, Y. X. ZHENG, H. M. ZENG, R. WALTER and K. FRIEDRICH, *Polymer* **42** (2001) 167.
23. Y. LIU, J. Y. LEE and L. HONG, *J. Power Sources* **109** (2002) 507.
24. C. J. R. VERBEEK, *Materials Letters* **57** (2003) 1919.
25. Z. WEN, T. ITOH, T. UNO, M. KUBO and O. YAMAMOTO, *Solid State Ionics* **8916** (2003) 1.
26. M. HASHIMOTO, H. TAKADAMA, M. MIZUNO, Y. YASUTOMI and T. KOKUBO, *Key Engineering Materials* **240–242** (2003) 415.
27. H. TAKADAMA, M. HASHIMOTO, Y. TAKIGAWA, M. MIZUNO, Y. YASUTOMI and T. KOKUBO, *Key Engineering Materials* **240–242** (2003) 951.
28. H. TAKADAMA, M. HASHIMOTO, Y. TAKIGAWA, M. MIZUNO, Y. YASUTOMI and T. KOKUBO, *Key Engineering Materials* **254–256** (2004) 569.
29. S. WEINER, *CRC Crit. Rev. Biochem*. **20** (1986) 365–408.
30. H. TAKADAMA, H. M. KIM, T. KOKUBO and T. NAKAMURA, *J. Biomed. Mater. Res*. **55** (2001) 185.
31. H. TAKADAMA, H. M. KIM, T. KOKUBO and T. NAKAMURA, *J. Biomed. Mater. Res*. **57** (2001) 441.